A NOVEL IMPLEMENTATION OF MODIFIED MAXWELL'S EQUATIONS IN THE PERIODIC FINITE-DIFFERENCE TIME-DOMAIN METHOD

G. Zheng, A. A. Kishk, A. W. Glisson, and A. B. Yakovlev

Department of Electrical Engineering
Center for Applied Electromagnetic Systems Research (CAESR)
University of Mississippi
University, MS 38677, USA

Abstract—To model periodic structures with oblique incident waves/scan angles in FDTD, the field transformation method is successfully used to analyze their characteristics. In the field transformation method, Maxwell's equations are Floquet-transformed so that only a single period of infinite periodic structure can be modeled in FDTD by using periodic boundary conditions (PBCs). A new discretization method based on the exponential time differencing (ETD) algorithm is proposed here for the discretization of the modified Maxwell's equations in the periodic FDTD method. This new discretization method provides an alternative way to discretize the modified Maxwell's equations with simpler updating forms that requires less CPU time and memory than the traditional stability factor method (SFM). These two methods have the same numerical accuracy and stability in the periodic FDTD method. Some validation cases are provided showing perfect match between the results of both methods.

1. INTRODUCTION

The finite-difference time-domain (FDTD) method has become one of the most popular numerical methods for the analysis of electromagnetic scattering, radiation, and propagation problems since Yee first introduced in 1966 [1]. In principle, this technique separates the electric and magnetic fields in Maxwell's curl equations at each time step, and the fields are determined at every cell point numerically in an established computational domain. The electric field intensity E and magnetic field intensity H at each cell point and each time step are computed during the simulation subject to zero initial

conditions. The updating equations in FDTD are simple, yet they have the capability to model geometrically complicated electromagnetic problems that are very complicated if analyzed by other methods. Besides these aforementioned advantages, it can also easily handle material inhomogeneities.

Periodic structures have received considerable attention in electromagnetic applications such as frequency selective surfaces (FSS) [2], electromagnetic bandgap (EBG) structures [3], and infinite antenna arrays [4]. These structures have such fine details at the element level that an accurate model must be provided to predict the correct electromagnetic behavior [5]. Because the entire structure is incorporated with the periodic characteristics, it is computationally unmanageable in the conventional FDTD method. Considering the fact that the overall structure consists of many replicas of the basic element (unit cell), one way to eliminate the computational burden is to model only a single-period structure with the proper periodic boundary conditions (PBCs) to simulate the effect of periodic replication in the periodic FDTD method [5]. In order to apply the FDTD method to the oblique incidence/scanning case in the single-period structure, the field transformation method was first introduced in [6] and its further extensions were presented in [7, 8]. In the field transformation method, the field components in Maxwell's equations are transferred from the E-H domain to the mapped P-Q domain and modified Maxwell's equations are formed. The difficulties in the implementation of time-advance and time-delay across the grid in the conventional FDTD method can be easily overcome by the field transformation method. Some extra terms due to the field transformations make direct implementation of the modified Maxwell's equations impossible in the periodic FDTD method. Several implementations in the periodic FDTD method have been presented in [7–12] to overcome this problem. One of these is the split-field method, which can be generalized to model lossy problems involving three-dimensional periodic structures [11]. In the split-field method, each field component is further split and a "two time-step updating" algorithm is used to update all the field components in the periodic FDTD method. To discretize the modified Maxwell's equations in the split-field method, the stability factor method (SFM) was introduced. This method uses a stability factor, which varies with the incident/scan angle, to achieve a numerically stable solution in the periodic FDTD method and it has been successfully used to analyze a variety of periodic structures [13].

In the proposed method, a new discretization method based on the exponential time differencing (ETD) algorithm is introduced to achieve the same numerical stability and accuracy in the periodic

FDTD method [14]. Compared to SFM, the ETD algorithm has simpler updating forms, and it requires less CPU time and memory. Several validation cases are provided and excellent agreements between these two methods among all of the validation cases are obtained.

2. FORMULATIONS

Consider a periodic structure that may contain lossy anisotropic materials with periodicities in both the y- and z-directions, and that is truncated by perfectly matched layer (PML) ABCs in the x-direction. In the frequency domain, the field transformation method is applied to transform the electric and magnetic field components from the E-H domain to the P-Q domain as,

$$\tilde{P}\left\{\begin{matrix} x \\ y \\ z \end{matrix}\right\} = \tilde{E}\left\{\begin{matrix} x \\ y \\ z \end{matrix}\right\} e^{j\Lambda\cdot\boldsymbol{\rho}}, \tag{1a}$$

$$\tilde{Q}\left\{\begin{matrix} x \\ y \\ z \end{matrix}\right\} = \eta_0\tilde{H}\left\{\begin{matrix} x \\ y \\ z \end{matrix}\right\} e^{j\Lambda\cdot\boldsymbol{\rho}}. \tag{1b}$$

The tilde symbol "$\sim$" is used to denote the field components in the frequency domain, $\Lambda = \hat{y}k_y + \hat{z}k_z$, and $\boldsymbol{\rho} = \hat{y}y + \hat{z}z$. After substituting these transformed field components into Maxwell's equations and transforming them from the frequency domain to the time domain, the modified time-dependent Maxwell's equations can be obtained [7, 8] (derivations are given in Appendix A),

$$\frac{\partial}{\partial t}\left(\frac{\varepsilon_r}{c}\vec{P} + \frac{1}{c}\Lambda \times \vec{Q}\right) = \nabla \times \vec{Q} - \vec{R} \tag{2a}$$

$$\frac{\partial}{\partial t}\left(\frac{\mu_r}{c}\vec{Q} - \frac{1}{c}\Lambda \times \vec{P}\right) = -\nabla \times \vec{P} - \vec{R}_m \tag{2b}$$

where $\vec{P} = P_x\hat{x} + P_y\hat{y} + P_z\hat{z}$, $\vec{Q} = Q_x\hat{x} + Q_y\hat{y} + Q_z\hat{z}$, $k_y = \sin\theta\phi$, $k_z = \cos\theta$, $\vec{R} = \sigma\eta_0\vec{P}$, $\vec{R}_m = \sigma^*/\eta_0\vec{Q}$, and θ, ϕ represent the incident/scan angles.

Expanding Equation (2) in time domain yields,

$$\frac{\varepsilon_{xr}}{c}\frac{\partial P_x}{\partial t} + \sigma_x\eta_0 P_x = \frac{\partial Q_z}{\partial y} - \frac{\partial Q_y}{\partial z} - \frac{k_y}{c}\frac{\partial Q_z}{\partial t} + \frac{k_z}{c}\frac{\partial Q_y}{\partial t} \tag{3a}$$

$$\frac{\varepsilon_{yr}}{c}\frac{\partial P_y}{\partial t} + \sigma_y\eta_0 P_y = -\frac{\partial Q_z}{\partial x} + \frac{\partial Q_x}{\partial z} - \frac{k_z}{c}\frac{\partial Q_x}{\partial t} \tag{3b}$$

$$\frac{\varepsilon_{zr}}{c}\frac{\partial P_z}{\partial t} + \sigma_z \eta_0 P_z = \frac{\partial Q_y}{\partial x} - \frac{\partial Q_x}{\partial y} + \frac{k_y}{c}\frac{\partial Q_x}{\partial t} \tag{3c}$$

$$\frac{\mu_{xr}}{c}\frac{\partial Q_x}{\partial t} + \frac{\sigma_x^*}{\eta_0}Q_x = -\frac{\partial P_z}{\partial x} + \frac{\partial P_y}{\partial z} + \frac{k_y}{c}\frac{\partial P_z}{\partial t} - \frac{k_z}{c}\frac{\partial P_y}{\partial t} \tag{3d}$$

$$\frac{\mu_{yr}}{c}\frac{\partial Q_y}{\partial t} + \frac{\sigma_y^*}{\eta_0}Q_y = \frac{\partial P_z}{\partial x} - \frac{\partial P_x}{\partial z} + \frac{k_z}{c}\frac{\partial P_x}{\partial t} \tag{3e}$$

$$\frac{\mu_{zr}}{c}\frac{\partial Q_z}{\partial t} + \frac{\sigma_z^*}{\eta_0}Q_z = -\frac{\partial P_y}{\partial x} + \frac{\partial P_x}{\partial y} - \frac{k_y}{c}\frac{\partial P_x}{\partial t}. \tag{3f}$$

Some extra terms shown on the right hand side (RHS) of Equations (3) result from the transformation defined in (1). Direct implementation in the periodic FDTD method is impossible due the time derivative on both sides of Equation (3). In order to eliminate the time derivative on the RHS, a new set of variables, which contain the information of the components with the time derivative on the RHS, are introduced to split the total fields into several parts as,

$$P_x = P_{xa} + \frac{k_z}{\varepsilon_{xr}}Q_y - \frac{k_y}{\varepsilon_{xr}}Q_z \tag{4a}$$

$$Q_x = Q_{xa} - \frac{k_z}{\mu_{xr}}P_y + \frac{k_y}{\mu_{xr}}P_z \tag{4b}$$

$$P_y = P_{ya} - \frac{k_z}{\varepsilon_{yr}}Q_x \tag{4c}$$

$$Q_y = Q_{ya} + \frac{k_z}{\mu_{yr}}P_x \tag{4d}$$

$$P_z = P_{za} + \frac{k_y}{\varepsilon_{zr}}Q_x \tag{4e}$$

$$Q_z = Q_{za} - \frac{k_y}{\mu_{zr}}P_x. \tag{4f}$$

By substituting these variables into Equations (3), the final updating equations in the periodic FDTD method can be achieved,

$$\frac{\varepsilon_{xr}}{c}\frac{\partial P_{xa}}{\partial t} + \sigma_x \eta_0 P_{xa} = \frac{\partial Q_z}{\partial y} - \frac{\partial Q_y}{\partial z} + \frac{\sigma_x \eta_0 k_y}{\varepsilon_{xr}}Q_z - \frac{\sigma_x \eta_0 k_z}{\varepsilon_{xr}}Q_y \tag{5a}$$

$$\frac{\varepsilon_{yr}}{c}\frac{\partial P_{ya}}{\partial t} + \sigma_y \eta_0 P_{ya} = -\frac{\partial Q_z}{\partial x} + \frac{\partial Q_x}{\partial z} + \frac{\sigma_y \eta_0 k_y}{\varepsilon_{yr}}Q_x \tag{5b}$$

$$\frac{\varepsilon_{zr}}{c}\frac{\partial P_{za}}{\partial t} + \sigma_z \eta_0 P_{za} = \frac{\partial Q_y}{\partial x} - \frac{\partial Q_x}{\partial y} - \frac{\sigma_z \eta_0 k_y}{\varepsilon_{zr}}Q_x \tag{5c}$$

$$\frac{\mu_{xr}}{c}\frac{\partial Q_{xa}}{\partial t} + \frac{\sigma_x^*}{\eta_0}Q_{xa} = -\frac{\partial P_z}{\partial y} + \frac{\partial P_y}{\partial z} + \frac{\sigma_x^* k_y}{\eta_0 \mu_{xr}}P_z + \frac{\sigma_x^* k_z}{\eta_0 \mu_{xr}}P_y \tag{5d}$$

$$\frac{\mu_{yr}}{c}\frac{\partial Q_{ya}}{\partial t} + \frac{\sigma_y^*}{\eta_0}Q_{ya} = \frac{\partial P_z}{\partial x} - \frac{\partial P_x}{\partial z} - \frac{\sigma_y^* k_y}{\eta_0 \mu_{yr}}P_x \tag{5e}$$

$$\frac{\mu_{zr}}{c}\frac{\partial Q_{za}}{\partial t} + \frac{\sigma_z^*}{\eta_0}Q_{za} = -\frac{\partial P_y}{\partial x} + \frac{\partial P_x}{\partial y} + \frac{\sigma_z^* k_y}{\eta_0 \mu_{zr}}P_x. \tag{5f}$$

A "two time-step updating" algorithm can be used to update Equations (4) and (5). A description of this algorithm can be found in [5]. In the following, discretization of Equation (5a) in the periodic FDTD method is given in detail as an example. The other equations can be developed in a similar way. In [11], a stability factor β is introduced to achieve the modified time-averaging of the loss term in the left hand side (LHS) of Equations (5) as,

$$\frac{\varepsilon_{xr}}{c}\frac{P_{xa}|_{i,j,k}^{n+1} - P_{xa}|_{i,j,k}^n}{dt} + \sigma_x \eta_0 \left[\beta P_{xa}|_{i,j,k}^{n+1} + (1-2\beta)P_{xa}|_{i,j,k}^{n+1/2} + \beta P_{xa}|_{i,j,k}^n\right]$$
$$= \frac{Q_z|_{i,j,k}^{n+1/2} - Q_z|_{i,j-1,k}^{n+1/2}}{dy} - \frac{Q_y|_{i,j,k}^{n+1/2} - Q_y|_{i,j,k-1}^{n+1/2}}{dz}$$
$$+ \frac{\sigma_x \eta_0 k_y}{\varepsilon_{xr}}\frac{Q_z|_{i,j,k}^{n+1/2} + Q_z|_{i,j-1,k}^{n+1/2}}{2} - \frac{\sigma_x \eta_0 k_z}{\varepsilon_{xr}}\frac{Q_y|_{i,j,k}^{n+1/2} + Q_y|_{i,j,k-1}^{n+1/2}}{2} \tag{6}$$

where $\beta = 0.5/\sin^2\theta\cos^2\phi$.

Such treatment for the loss term is necessary to achieve numerical stability in the periodic FDTD method due to the reason that waves propagating in the lossy media decay exponentially, and the standard Yee time-stepping algorithm cannot be easily used to handle such rapid changes. In the SFM, the numerical stability is achieved with the cost of complicated updating forms and it requires additional computational resources. An alternative approach to handle the loss terms is the exponential time differencing (ETD) algorithm. In the ETD algorithm, the numerical solution to the inhomogeneous differential equation consists of two parts: a general solution of the homogeneous equation and a particular solution of the inhomogeneous equation. The solution of homogeneous equation corresponding to inhomogeneous Equation (5a)

$$\frac{\varepsilon_{xr}}{c}\frac{\partial P_{xa}}{\partial t} + \sigma_x \eta_0 P_{xa} = 0 \tag{7a}$$

can be easily obtained as

$$P_{xa_{\text{homog}}}(t') = C_1 e^{-\frac{\sigma_x \eta_0 c}{\varepsilon_{xr}}t'} \tag{7b}$$

where C_1 is a constant. Equation (7b) can be expressed over one time step as follows,

$$P_{xa_{\text{homog}}}^{n+1}(t') = e^{-\frac{\sigma_x \eta_0 c}{\varepsilon_{xr}}\Delta t} P_{xa_{\text{homog}}}^{n}. \tag{7c}$$

The particular solution of Equation (5a) is given by

$$\begin{aligned}
P_{xa_{part}}(t') &= \frac{1}{\sigma_x \eta_0}\left(\frac{\partial Q_z}{\partial y} - \frac{\partial Q_y}{\partial z} + \frac{\sigma_x \eta_0 k_y}{\varepsilon_{xr}}Q_z - \frac{\sigma_x \eta_0 k_z}{\varepsilon_{xr}}Q_y\right) \\
&\quad + K e^{\frac{\sigma_x \eta_0 c}{\varepsilon_{xr}}t'} \tag{7d}
\end{aligned}$$

where K is a constant that needs to be determined subject to the initial conditions. In the periodic FDTD method, before any iteration, all the field components in the computational domain are initialized to zero. Therefore, the initial condition for the field component P_{xa} is given as

$$P_{xa_{part}}(t' = 0) = 0. \tag{7e}$$

By solving Equation (7e), constant K can be easily obtained, as given by

$$K = -\frac{1}{\sigma_x \eta_0}\left(\frac{\partial Q_z}{\partial y} - \frac{\partial Q_y}{\partial z} + \frac{\sigma_x \eta_0 k_y}{\varepsilon_{xr}}Q_z - \frac{\sigma_x \eta_0 k_z}{\varepsilon_{xr}}Q_y\right). \tag{7f}$$

After one time step increment, Δt, the particular solution can be obtained as

$$\begin{aligned}
P_{xa_{part}}(t' = \Delta t) &= \frac{1}{\sigma_x \eta_0}\left(1 - e^{\frac{\sigma_x \eta_0 c}{\varepsilon_{xr}}\Delta t}\right) \\
&\quad \times \left(\frac{\partial Q_z}{\partial y} - \frac{\partial Q_y}{\partial z} + \frac{\sigma_x \eta_0 k_y}{\varepsilon_{xr}}Q_z - \frac{\sigma_x \eta_0 k_z}{\varepsilon_{xr}}Q_y\right). \tag{7g}
\end{aligned}$$

With the obtained general solution of the homogeneous equation and a particular solution of the inhomogeneous equation, the overall solution of Equation (5a) can be easily obtained by superposition. The discretized form of the solution of Equation (5a) in the periodic FDTD method is given by

$$\begin{aligned}
P_{xa}^{n+1} &= P_{xa}^{n} e^{-\frac{\sigma_x \eta_0 c}{\varepsilon_{xr}}\Delta t} + \frac{1}{\sigma_x \eta_0}\left(1 - e^{-\frac{\sigma_x \eta_0 c}{\varepsilon_{xr}}\Delta t}\right) \\
&\quad \left[\begin{array}{c}
\left(\frac{1}{\Delta y} + \frac{\sigma_x \eta_0 k_y}{2\varepsilon_{xr}}\right) Q_z|_{i,j,k}^{n+1/2} - \left(\frac{1}{\Delta y} - \frac{\sigma_x \eta_0 k_y}{2\varepsilon_{xr}}\right) Q_z|_{i,j-1,k}^{n+1/2} \\
- \left(\frac{1}{\Delta z} + \frac{\sigma_x \eta_0 k_z}{2\varepsilon_{xr}}\right) Q_y|_{i,j,k}^{n+1/2} + \left(\frac{1}{\Delta z} - \frac{\sigma_x \eta_0 k_z}{2\varepsilon_{xr}}\right) Q_y|_{i,j,k-1}^{n+1/2}
\end{array}\right]. \tag{8}
\end{aligned}$$

Comparing the updating Equations (6) and (8), one finds an extra term in Equation (6), which requires more memory and computational time.

In the ETD algorithm, the numerical stability in the periodic FDTD method is the same as the SFM since both of these two discretization methods are based on the split-field set of Equation (5).

3. NUMERICAL VALIDATION

In this section, numerical validations based on the formulations described in Section 2 are presented. In the first numerical experiment, we consider a y- and z-periodic infinite infinitesimal dipole array with a $45°$ scan angle above an infinite perfect electric conducting (PEC) ground plane. In this validation case, both the zero conductivity (free space) and infinite conductivity (PEC) media types are considered. The grid sizes in the x, y, and z directions are $0.5\,\text{mm}$, and the time step is $0.42\,\text{ps}$. The computational domain in the x, y, and z directions is $15\,\text{cm} \times 15\,\text{cm} \times 15\,\text{cm}$ ($30 \times 30 \times 30$ cells). A horizontal y-polarized infinitesimal dipole is placed in the center of the computational domain $(15, 15, 15)$ and 12 cells above the infinite ground plane, with a Gaussian waveform excitation of the form

$$P_y(t) = \exp\left(-\frac{(t - t_0)^2}{\tau^2}\right) \qquad (9)$$

where t_0 is the time at which the pulse reaches its maximum and τ is a parameter related to pulse width. The sampling position for the electric field is placed at 10 cells away from the source position.

Fig. 1 shows the time-domain response obtained from the ETD algorithm and the SFM for an infinite dipole array with a $45°$ scan angle above an infinite ground plane. In Fig. 1, it can be noticed that the results obtained from these two methods appear to agree very well. In fact, the results obtained by the ETD algorithm agree with those obtained by the SFM up to the seventh digit. The strong fields shown in Fig. 1 before $1.5\,\text{ns}$ are contributed by the radiating fields propagating directly from the dipole elements and the scatter fields reflected from an infinite PEC ground plane. The computational time and memory requirements based on 10000 time steps for the ETD algorithm and the SFM are shown in Table 1.

A second numerical validation is conducted with the same computational domain, grid size, excitation form, time increment, and sampling positions as in the previous example. The only difference is that an infinite dielectric slab with permittivity $\varepsilon_r = 2.2$, permeability $\mu_r = 1$, and thickness $4\,\text{mm}$ is used to replace the infinite PEC ground
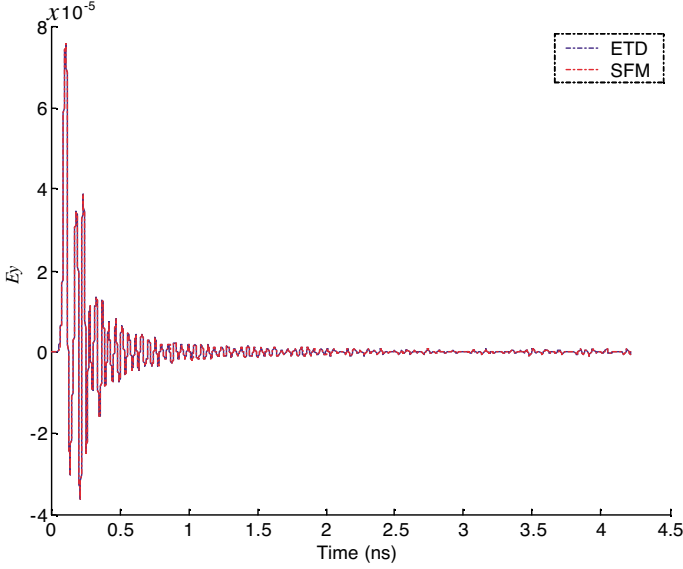
Figure 1. Time-domain response from the ETD algorithm and the SFM for an infinite infinitesimal-dipole array with a 45° scan angle above an infinite ground plane.

Table 1. The computational time and memory requirement for the ETD algorithm and the SFM.

	ETD	SMF
CPU time (min)	20	22
Memory (Mb)	19	19.5

plane. Different conductivities in the dielectric slab are used to validate the ETD algorithm.

Fig. 2 shows the time-domain responses obtained from the ETD algorithm and the SFM for an infinite dipole array with a 45° scan angle above an infinite dielectric slab. In the case of zero conduction loss, the periodic characteristics of the overall structure can be clearly noticed by the strong repeated pulses for the later time steps as shown in Fig. 1(a). Zero conduction loss in the substrate allows for the unattenuated propagation of surface waves in the dielectric slab. Therefore, pulses shown in the later time are resulting from these modes of the unit cells that are far away from the current unit cell. In
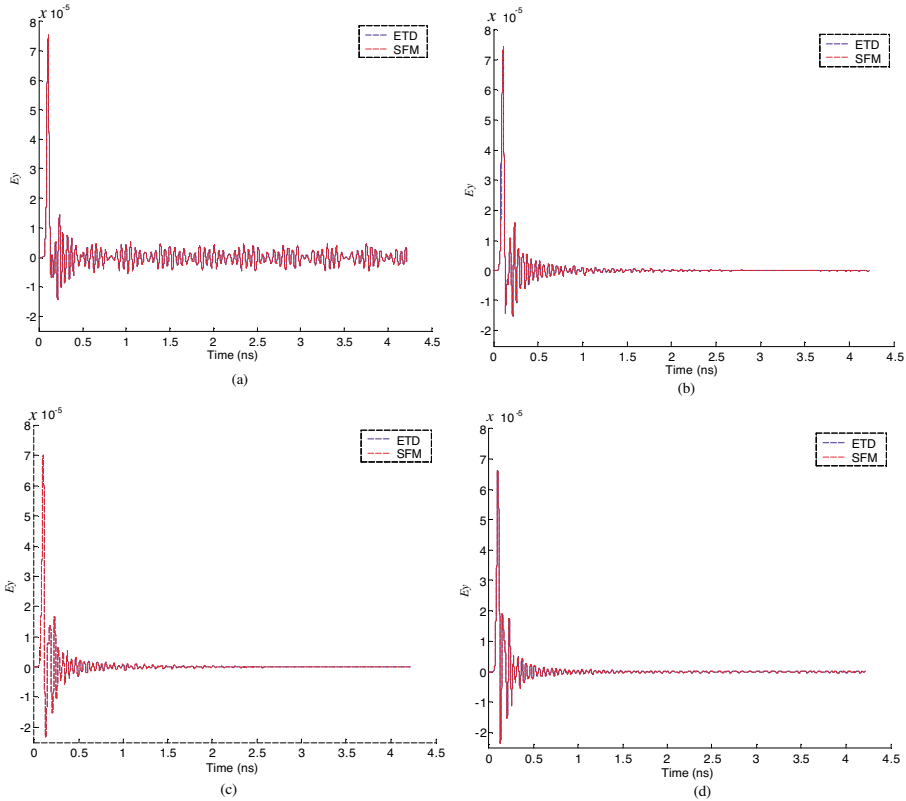
Figure 2. Time-domain response from the ETD algorithm and the SFM for an infinite dipole array with a 45° scan angle above an infinite dielectric slab with conductivities: (a) $\sigma = 0$, (b) $\sigma = 1$, (c) $\sigma = 10$, and (d) $\sigma = 100$.

the presence of conduction loss, surface waves in the infinite dielectric slab decay exponentially in the later time as shown in Fig. 2(b), (c), (d).

   To further test the numerical stability of the ETD algorithm, a material with high value of dielectric constant and conductivity should be used for this purpose. Hence, an additional stability test is performed for the case of a material with dielectric constant of 300 and conductivity of 300. The iteration steps in FDTD are chosen to be 10000, which is long enough to observe any divergence in the time domain for such a small computational domain. Fig. 3 shows the time-domain responses obtained from the ETD algorithm and
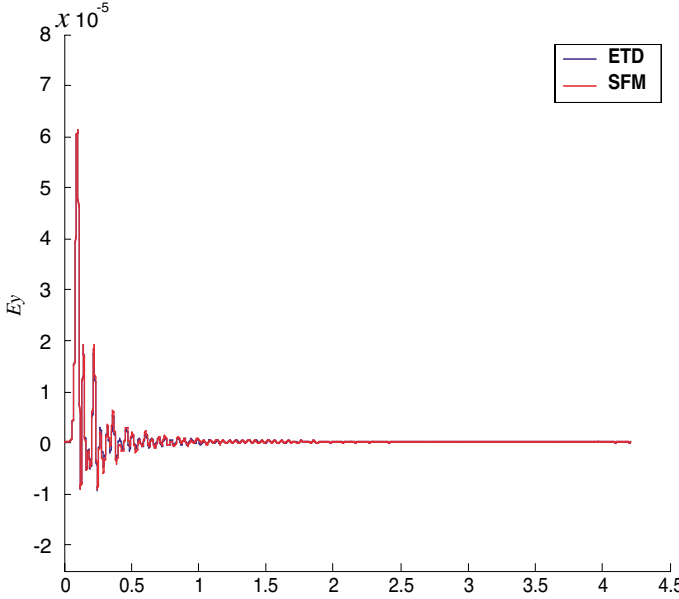
Figure 3. Time-domain responses obtained from the ETD algorithm and the SFM for an infinite dipole array with a 45° scan angle above a infinite dielectric slab with high dielectric constant and conductivity.

the SFM for an infinite dipole array with a 45° scan angle above an infinite dielectric slab with high dielectric constant and conductivity. No divergence phenomenon is observed. The ETD algorithm is thus shown to achieve the same stability as the SFM for high dielectric constant and conductivity material.

The last numerical validation is conducted with a coax-fed infinite rectangular dielectric resonator antenna (DRA) array above a PEC ground plane. The permittivity inside each rectangular DRA is chosen to be $\varepsilon_r = 12$. The geometry of a single element is shown in Fig. 4 and its dimensions (in mm) are: $a = b = 5.4 \, \text{mm}$ and $h = 7 \, \text{mm}$. The unit cell size for each element is 22.86 mm and 10.16 mm, in the x- and y-direction, respectively. The coax transmission line under the PEC ground plane is designed to 50 Ω characteristic impedance. The length of the probe, which is extended inside the rectangular DRA, is $Lp = 3.5 \, \text{mm}$ and it is offset 1.5 mm from the center of the rectangular DRA so that the proper mode can be excited [15]. Fig. 5 shows the time-domain responses of sampled voltage and current obtained from the ETD algorithm and the SFM with a 45° scan angle. The active input impedance at the coax port is plotted in Fig. 6, and is compared
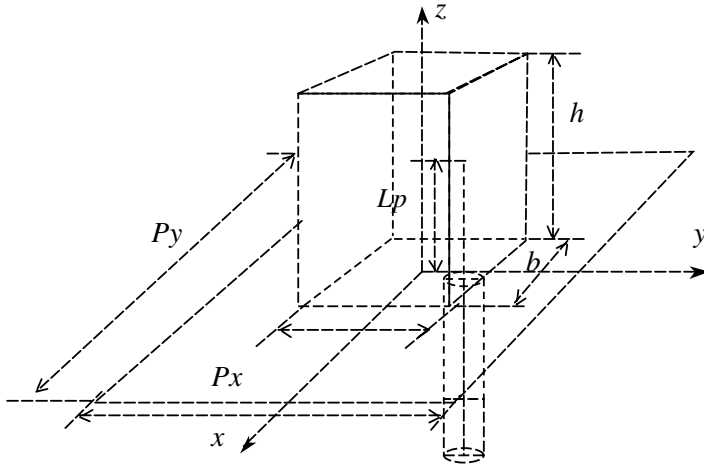
Figure 4. Geometry of a single element in an infinite rectangular DRA array.

with the results obtained from HFSS. Good agreement can be found between the results obtained from the ETD algorithm and HFSS except for some frequency points. In FDTD, the cell size determines the accuracy of the simulation. The smaller the cell, the more accurate one may expect the result to be. Theoretically, the cell size could approach zero to get the exact solution, but in practice, the cell size cannot be too small because of the limitations on the computational resources and cost. Due to the limitations on the cell size and the required conditions for the thin wire approximations, the model in FDTD could have some errors. These errors do not have a significant effect in a single element environment, while they do in infinite array environment since the active input impedance for each element is very sensitive to its surrounding environment. Thus, differences can be observed between the ETD algorithm and HFSS in Fig. 6.

A novel implementation of the modified Maxwell's equations in the periodic FDTD method was presented. By using the new discretization method based on the ETD algorithm, simpler updating forms and less CPU time and memory were obtained. At the same time, the new discretization method provides the same accuracy and has the same numerical stability as the SFM. Good agreement is obtained in all of the validation cases. The new discretization method based on the ETD algorithm provides a fast and accurate way to analyze electromagnetic behavior of periodic structures.
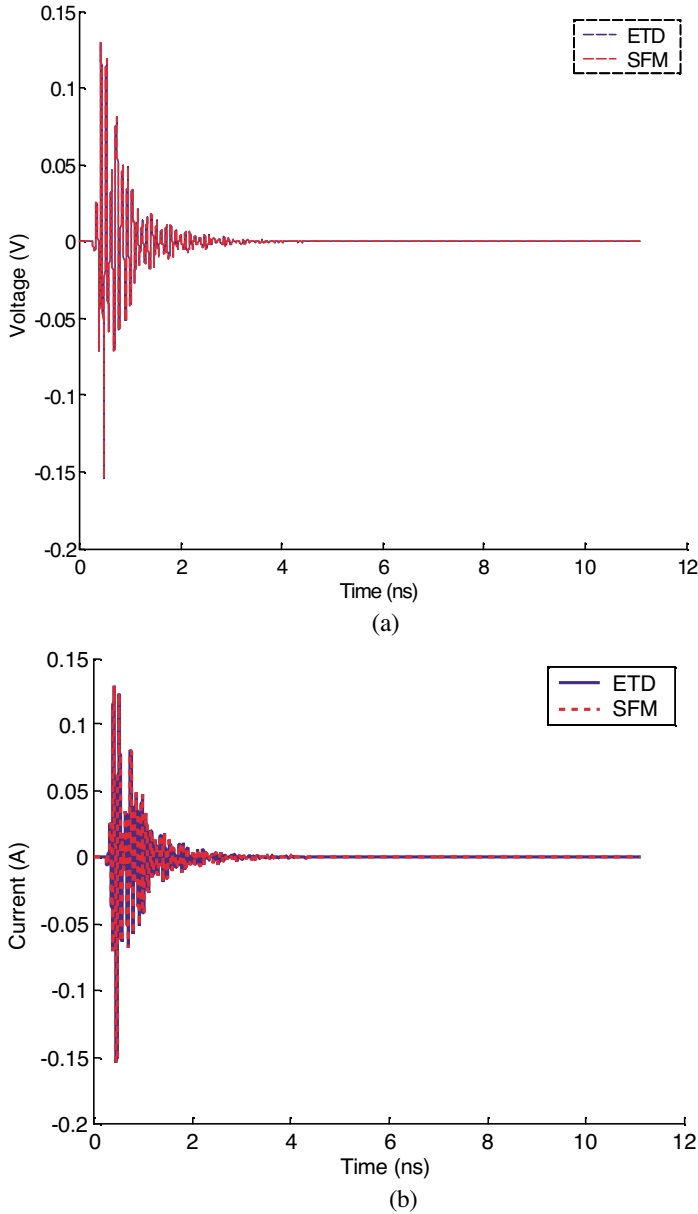
Figure 5. Time-domain response from the ETD algorithm and the SFM for an infinite rectangular DRA array with a 45° scan angle: (a) sampled voltage and (b) sampled current.
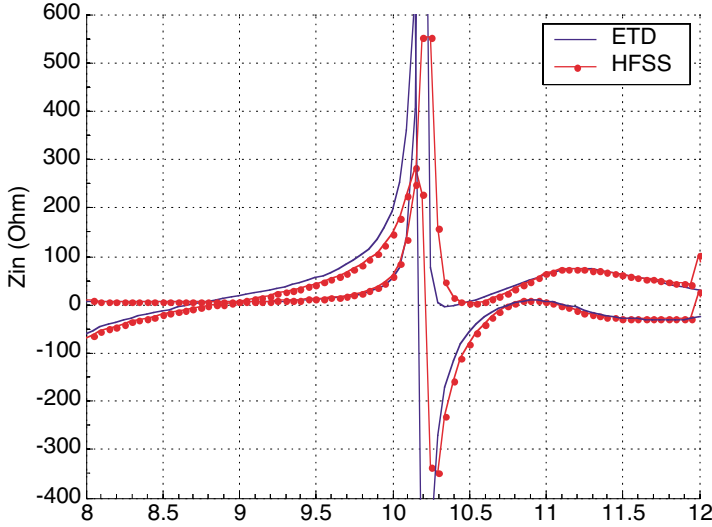
Figure 6. Comparison between the results obtained from the ETD algorithm and HFSS for the coupled input impedance of a single element in an infinite rectangular DRA array referenced at the coaxial port.

ACKNOWLEDGMENT

APPENDIX A. MODIFIED MAXWELL'S EQUATIONS IN THE P-Q DOMAIN

Define the transformed fields as

$$\tilde{P}_{\left\{\begin{array}{c} x \\ y \\ z \end{array}\right\}} = \tilde{E}_{\left\{\begin{array}{c} x \\ y \\ z \end{array}\right\}} e^{j\Lambda\cdot\boldsymbol{\rho}}, \tag{A1a}$$

$$\tilde{Q}_{\left\{\begin{array}{c} x \\ y \\ z \end{array}\right\}} = \eta_0 \tilde{H}_{\left\{\begin{array}{c} x \\ y \\ z \end{array}\right\}} e^{j\Lambda\cdot\boldsymbol{\rho}}. \tag{A1b}$$

These are used in the frequency domain Maxwell's equations to yield

$$\frac{j\omega\varepsilon_{xr}}{c}\tilde{P}_x + \sigma_x\eta_0\tilde{P}_x = \frac{\partial \tilde{Q}_z}{\partial y} - \frac{\partial \tilde{Q}_y}{\partial z} - j\vec{k}_y\frac{\partial}{\partial t}\tilde{Q}_z + j\vec{k}_z\tilde{Q}_y \tag{A2a}$$

$$\frac{j\omega\varepsilon_{yr}}{c}\tilde{P}_y + \sigma_y\eta_0\tilde{P}_y \;=\; -\frac{\partial\tilde{Q}_z}{\partial x} + \frac{\partial\tilde{Q}_x}{\partial z} - j\vec{k}_z\tilde{Q}_x \tag{A2b}$$

$$\frac{j\omega\varepsilon_{zr}}{c}\tilde{P}_z + \sigma_z\eta_0\tilde{P}_z \;=\; \frac{\partial\tilde{Q}_y}{\partial x} - \frac{\partial\tilde{Q}_x}{\partial y} + j\vec{k}_y\tilde{Q}_x \tag{A2c}$$

$$\frac{j\omega\mu_{xr}}{c}\tilde{Q}_x + \frac{\sigma_x^*}{\eta_0}\tilde{Q}_x \;=\; -\frac{\partial\tilde{P}_z}{\partial y} + \frac{\partial\tilde{P}_y}{\partial z} + j\vec{k}_y\tilde{P}_z - j\vec{k}_z\tilde{P}_y \tag{A2d}$$

$$\frac{j\omega\mu_{yr}}{c}\tilde{Q}_y + \frac{\sigma_y^*}{\eta_0}\tilde{Q}_y \;=\; \frac{\partial\tilde{P}_z}{\partial x} - \frac{\partial\tilde{P}_x}{\partial z} + j\vec{k}_z\tilde{P}_x \tag{A2e}$$

$$\frac{j\omega\mu_{zr}}{c}\tilde{Q}_z + \frac{\sigma_z^*}{\eta_0}\tilde{Q}_y \;=\; -\frac{\partial\tilde{P}_y}{\partial x} + \frac{\partial\tilde{P}_x}{\partial y} - \vec{k}_y\tilde{P}_x. \tag{A2f}$$

Transformation of Equations (A2) from the frequency domain to the time domain yields

$$\frac{\varepsilon_{xr}}{c}\frac{\partial P_x}{\partial t} + \sigma_x\eta_0 P_x \;=\; \frac{\partial Q_z}{\partial y} - \frac{\partial Q_y}{\partial z} - \frac{k_y}{c}\frac{\partial Q_z}{\partial t} + \frac{k_z}{c}\frac{\partial Q_y}{\partial t} \tag{A3a}$$

$$\frac{\varepsilon_{yr}}{c}\frac{\partial P_y}{\partial t} + \sigma_y\eta_0 P_y \;=\; -\frac{\partial Q_z}{\partial x} + \frac{\partial Q_x}{\partial z} - \frac{k_z}{c}\frac{\partial Q_x}{\partial t} \tag{A3b}$$

$$\frac{\varepsilon_{zr}}{c}\frac{\partial P_z}{\partial t} + \sigma_z\eta_0 P_z \;=\; \frac{\partial Q_y}{\partial x} - \frac{\partial Q_x}{\partial y} + \frac{k_y}{c}\frac{\partial Q_x}{\partial t} \tag{A3c}$$

$$\frac{\mu_{xr}}{c}\frac{\partial Q_x}{\partial t} + \frac{\sigma_x^*}{\eta_0}Q_x \;=\; -\frac{\partial P_z}{\partial y} + \frac{\partial P_y}{\partial z} + \frac{k_y}{c}\frac{\partial P_z}{\partial t} - \frac{k_z}{c}\frac{\partial P_y}{\partial t} \tag{A3d}$$

$$\frac{\mu_{yr}}{c}\frac{\partial Q_y}{\partial t} + \frac{\sigma_y^*}{\eta_0}Q_y \;=\; \frac{\partial P_z}{\partial x} - \frac{\partial P_x}{\partial z} + \frac{k_z}{c}\frac{\partial P_x}{\partial t} \tag{A3e}$$

$$\frac{\mu_{zr}}{c}\frac{\partial Q_z}{\partial t} + \frac{\sigma_z^*}{\eta_0}Q_z \;=\; -\frac{\partial P_y}{\partial x} + \frac{\partial P_x}{\partial y} - \frac{k_y}{c}\frac{\partial P_x}{\partial t} \tag{A3f}$$

where $\hat{k} = \sin\theta\cos\phi\hat{x} + \sin\theta\sin\phi\hat{y} + \cos\theta\hat{z} = k_x\hat{x} + k_y\hat{y} + k_z\hat{z}$.

By rewriting Equation (A3), a compact form of the modified Maxwell's equations in the time domain can be obtained as

$$\frac{\partial}{\partial t}\left(\frac{\varepsilon_r}{c}\vec{P} + \frac{1}{c}\Lambda\times\vec{Q}\right) \;=\; \nabla\times\vec{Q} - \vec{R} \tag{A4a}$$

$$\frac{\partial}{\partial t}\left(\frac{\mu_r}{c}\vec{Q} - \frac{1}{c}\Lambda\times\vec{P}\right) \;=\; -\nabla\times\vec{P} - \vec{R}_m. \tag{A4b}$$

REFERENCES

1. Yee, K. S., "Numerical solution of initial boundary value problems involving Maxwell's equations in isotropic media," *IEEE Trans. Antennas Propagat.*, Vol. AP-14, No. 3, 302–307, 1966.

2. Munk, B. A., *Frequency Selective Surfaces: Theory and Design,* John Wiley, New York, 2000.

3. Yablonovitch, E., "Photonic band-gap structures," *J. Opt. Soc. Amer. B.,* Vol. 10, No. 2, 283–294, 1993.

4. Maloney, J. G. and M. P. Kesler, "Analysis of antenna arrays using the split-field update FDTD method," *Proc. IEEE AP-S Int. Symp.,* Vol. 4, 2036–2039, 1998.

5. Taflove, A. and S. C. Hagness, *Computational Electromagnetics: the Finite-Difference Time-Domain Method,* 2nd ed., Artech House, Norwood, 2000.

6. Veysoglu, M. E., R. T. Shin, and J. A. Kong, "A finite-difference time-domain analysis of wave scattering from periodic surfaces: oblique incident case," *J. Electromagnetic Waves and Applications,* Vol. 7, No. 12, 1595–1607, 1993.

7. Kao, Y. C. A. and R. G. Atkins, "A finite difference-time domain approach for frequency selective surfaces at oblique incidence," *Proc. IEEE AP-S Int. Symp.,* Vol. 2, 1432–1435, 1996.

8. Kao, Y. C. A., "Finite-difference time domain modeling of oblique incidence scattering from periodic surfaces," Thesis, Massachusetts Institute of Technology, 1997.

9. Roden, J. A., "Electromagnetic analysis of complex structures using the fdtd technique in general curvilinear coordinates," Ph.D. Thesis, University of Kentucky, Lexington, KY, 1997.

10. Roden, J. A., S. D. Gedney, M. P. Kesler, J. G. Maloney, and P. H. Harms, "Time-domain analysis of periodic structures at oblique incidence: orthogonal and nonorthogonal FDTD implementations," *IEEE Trans. Microwave Theory Tech.,* Vol. 46, 420–427, 1998.

11. Harms, P. H., J. A. Roden, J. G. Maloney, M. P. Kesler, E. J. Kuster, and S. D. Gedney, "Numerical analysis of periodic structures using the split-field algorithm," *Proc. 13th Annual Review of Progress in Applied Computational Electromagnetics,* 104–111, 1997.

12. Aminian, A., F. Yang, and Y. Rahmat-Samii, "Bandwidth determination for soft and hard ground planes by spectral FDTD: a unified approach in visible and surface wave regions," *IEEE Trans. Antennas Propagat.,* Vol. 53, No. 1, 18–28, 2005.

13. Gedney, S. and U. Navsariwala, "An unconditional stable finite element time-domain solution of the vector wave equation," *IEEE Microwave Guided Wave Lett.,* Vol. 5, 332–334, Oct. 1995.

14. Holland, R., "Finite-difference time-domain (FDTD) analysis of

magnetic diffusion," *IEEE Trans. Electromagnetic Compatibility,* Vol. 36, 32–39, Feb. 1994.

15. Luk, K. M. and K. W. Leung, *Dielectric Resonator Antennas,* Research Studies Press, Bristol, 2003.